

Nonlinear diffusion and exclusion processes with contact interactionsAnthony E. Fernando, Kerry A. Landman,^{*} and Matthew J. Simpson*Department of Mathematics and Statistics, University of Melbourne, Victoria 3010, Australia*

(Received 9 September 2009; revised manuscript received 26 November 2009; published 11 January 2010)

Exclusion processes on a regular lattice are used to model many biological and physical systems at a discrete level. The average properties of an exclusion process may be described by a continuum model given by a partial differential equation. We combine a general class of contact interactions with an exclusion process. We determine that many different types of contact interactions at the agent-level always give rise to a nonlinear diffusion equation, with a vast variety of diffusion functions $D(C)$. We find that these functions may be dependent on the chosen lattice and the defined neighborhood of the contact interactions. Mild to moderate contact interaction strength generally results in good agreement between discrete and continuum models, while strong interactions often show discrepancies between the two, particularly when $D(C)$ takes on negative values. We present a measure to predict the goodness of fit between the discrete and continuous model, and thus the validity of the continuum description of a motile, contact-interacting population of agents. This work has implications for modeling cell motility and interpreting cell motility assays, giving the ability to incorporate biologically realistic cell-cell interactions and develop global measures of discrete microscopic data.

DOI: [10.1103/PhysRevE.81.011903](https://doi.org/10.1103/PhysRevE.81.011903)

PACS number(s): 87.10.Ed, 87.10.Hk, 87.17.Aa, 05.10.-a

I. INTRODUCTION

Exclusion processes are a class of lattice-based interacting random walk models where agents move and each lattice site is occupied by at most one agent [1,2]. Because each agent excludes all others from occupying the same position, exclusion processes are a natural choice to model real motility processes with applications including traffic flow [3], cell motility [4], and ecological applications [5].

Exclusion processes can be viewed from two different perspectives. Microscopic simulation data can be visualized, so that the movement of individual agents within the population can be tracked [6–8]. Alternatively, simulation data can be averaged—this data then correspond to a macroscopic continuum description of the system in terms of a partial differential equation (PDE) [1,6,9,10]. The construction of continuum models can be advantageous relative to the microscopic approach, since a PDE gives a global perspective of the system and is particularly attractive when considering large systems where repeated simulations are computationally infeasible.

Traditional averaging of symmetric exclusion processes (without bias) gives a linear diffusion equation [1]. Although agents interact with each other, the interactions are symmetric and cancel [9]. Therefore, these interactions do not appear in the macroscopic description of the system, given by a linear PDE [1]. More recently, an asymmetric simple exclusion process, with a biologically motivated contact-maintaining motility mechanism, was developed by Deroulers *et al.* [6]. The additional interactions led to a nonlinear diffusion equation.

Here, we extend the work of Deroulers *et al.* [6] to a broader range of biologically motivated mechanisms, accounting for contact-forming, contact-breaking, and contact-maintaining interactions. The contact interactions are consid-

ered within the framework of an exclusion process on a general d -dimensional lattice. Conservation arguments are used to derive continuum models, which are described by nonlinear diffusion equations. These nonlinear diffusion equations are validated for a range of two-dimensional lattices. We also develop simple tools to predict when the averaged discrete and continuum models match and when they differ.

The PDE models developed here support a range of complex behaviors. We can choose motility mechanisms leading to nonlinear diffusion functions $D(C)$, which are positive and either monotonically increasing or decreasing functions for all $C \in [0, 1]$, and others with even more features. Some contact interactions lead to nonlinear diffusion functions which are negative on some interval $(C_1, C_2) \in [0, 1]$. In these cases, the PDE models may give rise to solutions containing shocks [11].

II. DISCRETE MODEL

Motile agents move on an arbitrary d -dimensional periodic lattice with uniform spacing Δ . Agents can be viewed either as occupying sites or as residing in regions, since each site v is associated with a spatial region consisting of all points closer to site v than to any other. In two dimensions, these regions are polygonal tiles; the square lattice is associated with square tiles, while the triangular lattice is associated with hexagonal tiles.

Before describing various contact interaction mechanisms, we define various neighborhood sets.

A. Neighborhood sets

For any site v on a periodic lattice, we define five neighborhood sets.

(a) $\mathcal{N}\{v\}$ denotes the set of nearest-neighbor sites, that is, those sites one lattice-space distant from v . In the model,

*kerry.l@unimelb.edu.au

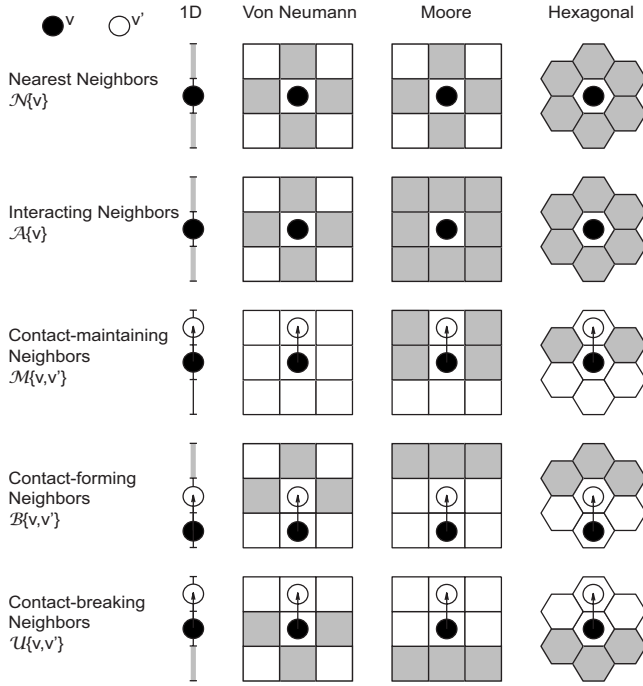


FIG. 1. Neighborhood sets for a one-dimensional and various two-dimensional lattices. Black markers depict the reference site v , white markers depict the target site $v' \in \mathcal{N}\{v\}$. The defined neighborhood set in each row is shaded gray. Note that in one-dimension and for the von Neumann neighborhood, $\mathcal{M}\{v, v'\} = \emptyset$.

these are the sites to which movements from site v can be attempted.

(b) $\mathcal{A}\{v\}$ denotes the set of sites whose occupants are in contact with an agent at v and potentially influence the movement of an agent at v . This neighborhood is referred to as the interacting neighborhood.

(c) $\mathcal{M}\{v, v'\}$ denotes the set of maintained sites in the interacting neighborhood when moving from site v to site $v' \in \mathcal{N}\{v\}$. Hence, $\mathcal{M}\{v, v'\} = \mathcal{A}\{v\} \cap \mathcal{A}\{v'\}$.

(d) $\mathcal{B}\{v, v'\}$ denotes the set of sites in the interacting neighborhood $\mathcal{A}\{v'\}$ gained in a move from v to v' , excluding the original site v . Hence, $\mathcal{B}\{v, v'\} = \mathcal{A}\{v'\} \setminus \{\mathcal{A}\{v\} \cup v\}$. This neighborhood is referred to as the contact-forming neighborhood.

(e) $\mathcal{U}\{v, v'\}$ denotes the set of sites in the interacting neighborhood $\mathcal{A}\{v\}$ lost in a move from v to v' , excluding the destination site v' . Hence, $\mathcal{U}\{v, v'\} = \mathcal{A}\{v\} \setminus \{\mathcal{A}\{v'\} \cup v'\}$. This neighborhood is referred to as the contact-breaking neighborhood. Symmetry considerations give $\mathcal{U}\{v, v'\} = \mathcal{B}\{v', v\}$.

Figure 1 illustrates each of these sets on four different lattices. Two variations on the square lattice are given—in both cases the nearest neighbors are the same, but there is a difference in the interacting neighborhoods. When the interacting neighborhood is a von Neumann neighborhood [12], then $\mathcal{A}\{v\} = \mathcal{N}\{v\}$. In contrast, when the interacting neighborhood is a Moore neighborhood [12], then $\mathcal{A}\{v\}$ comprises the four nearest neighbors together with the four diagonal neighbors. As shown, this choice of interacting neighborhood leads to distinctly different neighborhoods for the contact interactions, given by $\mathcal{M}\{v, v'\}$, $\mathcal{B}\{v, v'\}$, and $\mathcal{U}\{v, v'\}$.

The number of elements in a set \mathcal{Z} is denoted by $|\mathcal{Z}|$. In particular, the number of nearest neighbors of site v is $N = |\mathcal{N}\{v\}|$.

B. Exclusion process with contact interactions

A simple exclusion process [1,2] with random sequential updating [13] is implemented on the periodic lattice. If there are M agents on the lattice, then for each time step of duration τ , we make M sequential independent random choices of an agent. On average, each agent is chosen once per time step. When chosen, an agent is given the opportunity to move with probability P . Naturally, in an exclusion process, when an agent is chosen to move to a target site in $\mathcal{N}\{v\}$ that is already occupied, the move is aborted.

Consider an agent at site v which has been given an opportunity to move with probability P . We discuss two choices to accommodate contact interactions.

(1) *Determine direction and then contact interactions:* randomly choose a target site from $\mathcal{N}\{v\}$ with equal probability for each site. Then determine the contact interactions in terms of the neighborhood sets $\mathcal{M}\{v, v'\}$, $\mathcal{B}\{v, v'\}$, $\mathcal{U}\{v, v'\}$ and finally assign probabilities to complete the move. In implementing this method, two random numbers are generated per motile agent per move.

(2) *Determine contact interactions and then direction:* determine all the possible target site contact interactions in terms of the neighborhood sets and then determine the probability of movement to each site in $\mathcal{N}\{v\}$. In implementing this method, only one random number is generated per motile agent per move.

III. CONSERVATION EQUATION AND CONTINUUM MODEL

Instead of using a quantumlike formalism for master equations like in Deroulers *et al.* [6], here, we rely on standard conservation arguments to derive a continuum model [1]. The key steps in connecting our discrete model with a continuum model are outlined. We denote the occupancy of site v as C_v , with $C_v = 1$ for an occupied site and $C_v = 0$ for an empty site. Averaging over many statistically identical realizations, we write the average occupancy of site v as $\langle C_v \rangle$. This $\langle C_v \rangle$ can also be interpreted as the local probability of occupancy or the local density.

The change in average occupancy of site v during the time interval t to $t + \tau$ is denoted $\delta \langle C_v \rangle$. We let $T(v'|v)$ be the conditional transition probability that the agent will move from site v to site $v' \in \mathcal{N}\{v\}$ during τ . Then, the change in average occupancy due to a transition in a given direction is $T(v'|v) \langle C_v \rangle$. Summing all directions, we obtain the discrete conservation equation

$$\delta \langle C_v \rangle = \sum_{v' \in \mathcal{N}\{v\}} [T(v'|v) \langle C_{v'} \rangle - T(v|v') \langle C_v \rangle]. \quad (1)$$

Changes in average occupancy due to transitions into site v have a positive sign, while transitions out of site v have a negative sign. Since we interpret each factor in Eq. (1) as a probability, we are assuming that the occupancy of a lattice

site is independent of the occupancy of other lattice sites [1]. A similar assumption is implicit in developing each $T(v'|v)$ below. Equation (1) is the starting point for various continuum models that incorporate different types of contact interactions in the conditional probabilities $T(v'|v)$.

The discrete model is related to a PDE in the appropriate limit as $\Delta \rightarrow 0$ and $\tau \rightarrow 0$, where the discrete values of $\langle C_v \rangle$ are replaced by a continuous variable C . To do this, all terms in Eq. (1) are expanded in Taylor series about the particular site v , keeping terms up to $\mathcal{O}(\Delta^2)$. The truncated Taylor series are substituted into Eq. (1), and the expression is divided by τ . Taking limits as $\Delta \rightarrow 0$ and $\tau \rightarrow 0$ jointly, with the ratio Δ^2/τ held constant [14,15], in the continuum limit we obtain a nonlinear diffusion equation of the form

$$\frac{\partial C}{\partial t} = D_0 \nabla \cdot [D(C) \nabla C]. \quad (2)$$

Here, the free agent diffusivity is

$$D_0 = \frac{P}{2d} \lim_{\Delta, \tau \rightarrow 0} \left(\frac{\Delta^2}{\tau} \right), \quad (3)$$

where d is the dimension of the lattice. In the following sections, we will show that the diffusivity function $D(C)$ depends on the nature of the contact interactions and the lattice used in the discrete model.

IV. DIRECTION THEN INTERACTIONS

In the first method, there are N equally likely choices of target site from $\mathcal{N}\{v\}$. We consider contact-maintaining, contact-forming, and contact-breaking neighborhoods and determine the relevant $T(v'|v)$.

For the simple case when there are no agent interactions apart from exclusion, the conditional transition probability $T(v'|v)$ is the probability P/N of moving to any of the target sites v' multiplied by the probability that the destination site v' is vacant. Therefore,

$$T(v'|v) = \frac{P}{N} (1 - \langle C_{v'} \rangle). \quad (4)$$

In the continuum limit, we obtain a linear diffusion equation with $D(C)=1$ [1,10].

A. Contact-maintaining interactions

Recently, Deroulers *et al.* [6] investigated a specific type of contact interaction on a hexagonally tiled lattice in two dimensions and face-centered cubic and hexagonal close-packed lattices in three dimensions. The motility events were affected by the occupancy of sites in common between the occupied and target site (exactly our maintain neighborhood set $\mathcal{M}\{v, v'\}$). After choosing a direction, the move was completed with probability u if at least one of the two adjacent cells is occupied, and probability $(1-u)$ if both are unoccupied. Here, we confirm and generalize their results on an arbitrary d -dimensional lattice.

We require the occupancy of the contact-maintaining set $\mathcal{M}\{v, v'\}$ and express the probability that at least one mem-

ber is occupied as the complement that all are empty, namely,

$$P_{\mathcal{M}\{v, v'\}} = 1 - \prod_{m \in \mathcal{M}\{v, v'\}} (1 - \langle C_m \rangle). \quad (5)$$

Since the maintained neighbors being occupied or unoccupied are mutually exclusive events, we assign independent probabilities of movement in each instance. If we define the probability u of moving if at least one of the sites in $\mathcal{M}\{v, v'\}$ is occupied, and w if all are unoccupied, then the conditional transition probability is

$$T(v'|v) = \frac{P}{N} (1 - \langle C_{v'} \rangle) [u P_{\mathcal{M}\{v, v'\}} + w (1 - P_{\mathcal{M}\{v, v'\}})]. \quad (6)$$

Substituting this term into Eq. (1) and taking limits leads to Eq. (2) with

$$D(C) = u + (w - u)(1 - C)^m, \quad (7)$$

for $m = |\mathcal{M}\{v, v'\}|$. The nonlinear diffusion functions for a selection of lattices are given in Table I in the Appendix.

For the special case of $w=1-u$, Eq. (7) reduces to the results of Deroulers *et al.* [6] for the triangular lattice ($d=2, m=2$), and for the face-centered cubic and hexagonal close-packed lattice ($d=3, m=4$).

We note that regardless of the choices of probabilities u and w , $D(C)$ is non-negative on the interval $C \in [0, 1]$. When $w=u$, so there is no bias on maintaining contact neighbors, $D(C)$ is independent of C , so we again have a linear diffusion equation.

B. General contact-forming and contact-breaking interactions

Transitions from v to v' will result in some elements in the interacting neighborhood being gained and some being lost. We describe the four possible scenarios, depending on the occupancy of $\mathcal{B}\{v, v'\}$ and $\mathcal{U}\{v, v'\}$. Given a choice of v' , if all sites in both sets are unoccupied, then the motile agent will complete the move with probability s . If at least one contact-forming neighbor is occupied and the contact-breaking neighbors are unoccupied, this is a pure contact-forming move, and the probability of completing the move is p . Similarly, a pure contact-breaking move results when at least one contact-breaking neighbor is occupied and all contact-forming neighbors are unoccupied, and is completed with probability q . Finally, if at least one site is occupied in both the contact-forming and contact-breaking neighborhoods, then it is completed with probability r .

The probability $P_{\mathcal{B}\{v, v'\}}$ that at least one contact-forming site is occupied is the complement of the probability that all are empty. Likewise, the probability $P_{\mathcal{U}\{v, v'\}}$ can be defined. Thus,

$$P_{\mathcal{B}\{v, v'\}} = 1 - \prod_{b \in \mathcal{B}\{v, v'\}} (1 - \langle C_b \rangle),$$

$$P_{\mathcal{U}\{v, v'\}} = 1 - \prod_{u \in \mathcal{U}\{v, v'\}} (1 - \langle C_u \rangle). \quad (8)$$

The conditional transition probability is written as

$$\begin{aligned}
 T(v'|v) &= \frac{P}{N}(1 - \langle C_{v'} \rangle)[s(1 - P_{\mathcal{B}\{v,v'\}})(1 - P_{\mathcal{U}\{v,v'\}}) \\
 &\quad + pP_{\mathcal{B}\{v,v'\}}(1 - P_{\mathcal{U}\{v,v'\}}) + q(1 - P_{\mathcal{B}\{v,v'\}})P_{\mathcal{U}\{v,v'\}} \\
 &\quad + rP_{\mathcal{B}\{v,v'\}}P_{\mathcal{U}\{v,v'\}}]. \quad (9)
 \end{aligned}$$

Substituting this term into Eq. (1) and taking continuum limits leads to Eq. (2). The nonlinear diffusion function for a selection of lattices is given in Table I in the Appendix. If we define $\beta = |\mathcal{A}\{v\}| + 1$ and $k = |\mathcal{B}\{v, v'\}| = |\mathcal{U}\{v, v'\}|$, then

$$\begin{aligned}
 D(C) &= r + (s - p - q + r)(1 - C)^{2k} \\
 &\quad + [p(1 - \beta C) + q(1 + \beta C) - 2r](1 - C)^k. \quad (10)
 \end{aligned}$$

We note that $D(0) = s$ and $D(1) = r$.

It is useful to consider contact-forming or contact-breaking interactions in isolation. For contact-forming interactions alone, we take the general formulation and neglect the contact-breaking interactions by setting $q = s$ and $r = p$. With these restrictions, Eq. (10) simplifies to

$$D(C) = p + (s - p)(1 + \beta C)(1 - C)^k. \quad (11)$$

Since $D(0) = s$ and $D(1) = p$, the contact-forming probability dominates at high densities, and free movement probability dominates at low densities. When $p = s$, there is no bias toward or away from forming contacts and we obtain a linear diffusivity, $D(C) = s$, as expected.

Similarly, we consider the contact-breaking interactions alone by choosing $p = s$ and $r = q$. Substituting these values into Eq. (10) gives the contact-breaking diffusion function as

$$D(C) = q + (s - q)(1 - \beta C)(1 - C)^k. \quad (12)$$

Note that this is similar to Eq. (11), with only a change in sign in the linear factor in C . Now $D(0) = s$ and $D(1) = q$, while $q = s$ results in the constant $D(C) = s$.

Finally, we note that $D(C)$ in Eqs. (11) and (12) will have either a local minimum or maximum for $C \in [0, 1]$. Clearly, in the case of local minimum, values of C where $D(C) < 0$ will have interesting consequences.

C. Combined contact-forming or contact-breaking and contact-maintaining interactions

The general contact-forming or contact-breaking interactions may be combined with the contact-maintaining interactions. If the contact-maintaining interactions operate independently of the contact-forming and contact-breaking interactions, we define (i) u and w as the probabilities of moving if there are at least one or zero maintained neighbors, respectively, described in Sec. IV A, and (ii) p , q , r , and s are the probabilities for the contact-forming or contact-breaking interactions described in Sec. IV B. Then, the conditional probability is given by

$$\begin{aligned}
 T(v'|v) &= \frac{P}{N}(1 - \langle C_{v'} \rangle)[uP_{\mathcal{M}\{v,v'\}} + w(1 - P_{\mathcal{M}\{v,v'\}})] \\
 &\quad \times [s(1 - P_{\mathcal{B}\{v,v'\}})(1 - P_{\mathcal{U}\{v,v'\}}) \\
 &\quad + pP_{\mathcal{B}\{v,v'\}}(1 - P_{\mathcal{U}\{v,v'\}}) + q(1 - P_{\mathcal{B}\{v,v'\}})P_{\mathcal{U}\{v,v'\}} \\
 &\quad + rP_{\mathcal{B}\{v,v'\}}P_{\mathcal{U}\{v,v'\}}]. \quad (13)
 \end{aligned}$$

This generates

$$\begin{aligned}
 D(C) &= [u + (w - u)(1 - C)^m] \times \{r + (s - p - q + r)(1 - C)^{2k} \\
 &\quad + [p(1 - \beta C) + q(1 + \beta C) - 2r](1 - C)^k\}. \quad (14)
 \end{aligned}$$

It is interesting to note that this expression is simply a product of the $D(C)$ functions given by Eqs. (7) and (10).

Alternatively, if the contact-maintaining interactions do not operate independently of the contact-forming and contact-breaking interactions then we need to define different values for the contact-forming or contact-breaking interaction probabilities, depending on whether or not maintained neighbors participate in the move. In the usual way, we define probabilities p , q , r , and s if there are no maintained neighbors, and probabilities p^* , q^* , r^* , and s^* if at least one maintained neighbor is present. The resulting diffusion function is

$$\begin{aligned}
 D(C) &= [1 - (1 - C)^m][r^* + (s^* - p^* - q^* + r^*)(1 - C)^{2k} \\
 &\quad + (p^*(1 - \beta C) + q^*(1 + \beta C) - 2r^*)(1 - C)^k] \\
 &\quad + (1 - C)^m[r + (s - p - q + r)(1 - C)^{2k} \\
 &\quad + (p(1 - \beta C) + q(1 + \beta C) - 2r)(1 - C)^k]. \quad (15)
 \end{aligned}$$

D. In-line contact-forming and contact-breaking interactions

On any lattice where sites are arranged in lines, it is possible to restrict the interacting neighborhood for a given move to be the neighbors along the line in the direction of the move. The in-line neighborhood is then just that of the one-dimensional case shown in Fig. 1. Transition probability arguments for the in-line neighborhoods yields, in the continuum limit, the set of nonlinear diffusion functions for the one-dimensional line, tabulated in the third row in Table I in the Appendix. Of course, the dimension of the lattice still appears in the free agent diffusivity D_0 in Eq. (3). (Note that contact-maintaining rules are not applicable for in-line interactions.)

Our previous contact interaction neighborhoods gave lattice dependent $D(C)$ functions, since they involve the constants $m = |\mathcal{M}\{v, v'\}|$, $\beta = |\mathcal{A}\{v\}| + 1$, and/or $k = |\mathcal{B}\{v, v'\}| = |\mathcal{U}\{v, v'\}|$. When the interactions are applied to in-line neighborhoods, the $D(C)$ functions are lattice independent, since the interacting neighborhood, and hence k and β , are the same for all lattices.

V. COMPARING DISCRETE AND CONTINUUM RESULTS

To test the validity of our averaging arguments, we generate and compare results from the discrete and continuum

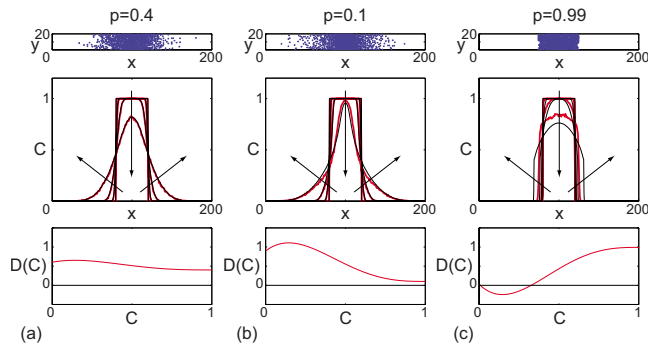


FIG. 2. (Color online) Transient results for contact-forming interactions on a hexagonal tiling ($k=3$, $\beta=7$) for various interaction strengths with $s=1-p$ for (a) $p=0.4$ (mildly repelling), (b) $p=0.1$ (strongly repelling), and (c) $p=0.99$ (very strongly attracting). Results in the top row show the distribution of agents in a single realization after 1000 time steps. The middle row compares the solution of the continuum model (black) and the averaged column density data (red) at $t=0, 10, 100, 1000$; arrows indicate the direction of increasing time. The bottom row shows the functional dependence of $D(C)$ on C (red) with $D(C)=0$ given by the horizontal line (black). All discrete data use $P=\Delta=\tau=1$ and averages are taken over 200 Monte Carlo realizations. Numerical solutions of the continuum models use $\delta x=0.5$ and $\delta t=0.1$. In (c), $D(C)<0$ for some values of C and the solutions of the continuum model have a discontinuity.

models for two kinds of simulations. First, we compare transient simulations describing the spreading of an initially close-packed population. Second, we compare steady state profiles describing the movement of agents between two reservoirs of a given density. For the transient simulation, we compare averaged simulation data to the numerical solution of Eq. (2), while for the steady problem, we compare averaged discrete data to an exact analytical solution of the associated boundary value problem.

Equation (2) is solved numerically with a finite difference method with constant grid spacing δx and implicit Euler stepping with constant time steps δt . Picard linearization, with tolerance ε , is used to solve the nonlinear equations. All one-dimensional continuum solutions presented in this work correspond to $\delta x=0.5$ and $\delta t=0.1$, and tolerance $\varepsilon=1 \times 10^{-6}$. This choice of δx gives grid-independent results.

A. Transient results

For the transient simulations, we consider a two-dimensional lattice, with spacing $\Delta=1$, of size 200×200 with periodic boundary conditions imposed on the horizontal boundaries and reflecting boundary conditions imposed on the vertical boundaries. All sites with $80 \leq x \leq 120$ are initially occupied with agents. This initial condition and the periodic boundary conditions reduce the system to a one-dimensional problem since no vertical structure is imposed by the initial agent distribution or the boundary conditions. Column-averaged density data, averaged over 200 identically prepared realizations [8,9] is compared with the solution of a one-dimensional form of Eq. (2).

The three columns in Fig. 2 illustrate a range of results for

contact-forming interactions on a hexagonal tiling. Results in Figs. 2(a) and 2(b) are for mildly repelling and strongly repelling cases, respectively, while Fig. 2(c) corresponds to a very strongly attracting case. Snapshots of the agents at $t=1000$ are given in the top row showing that the agents spread further from their initial location when the agents are more repelling. The solution of Eq. (2) is compared with column-averaged density profiles from the simulations in the middle row, showing a good correspondence between the simulation data and the continuum model for the cases $p=0.1$ and $p=0.4$. The density data for $p=0.99$ shows a divergence between the simulation data and the continuum model. Moreover, we observe the formation of discontinuous solutions of the continuum model for this case.

The transition from smooth solutions to discontinuous solutions of the nonlinear diffusion equations can be explained by investigating the functional dependence of $D(C)$, given in the bottom row of Fig. 2. For the first two columns, $D(C)>0$. In contrast, in the last column $D(C)<0$ for some values of C —this occurs for a sufficiently large contact-forming parameter p , corresponding to sufficiently strong agent adhesion. We note that the numerical solution of the PDE develops a shock, and that the values of C sampled correspond only to those where $D(C)>0$, as seen in the middle row in Fig. 2(c). The existence of discontinuous solutions of nonlinear diffusion equations has been previously analyzed [11]. More recently, Aanguige and Schmeiser [16] developed a continuous-time master equation representing cell motility with adhesion on a one-dimensional lattice. In the continuum limit, their discrete model gave a nonlinear diffusion equation where the diffusivity could be negative for sufficiently strong adhesion.

In addition to the contact-forming interactions shown in Fig. 2, we also find the comparison between the discrete and continuum models to be excellent for contact-breaking, general contact-forming/contact-breaking, and contact-maintaining interactions for a range of parameter values.

Finally, in Fig. 3, we present results for the contact-forming interaction model implemented on three different lattices, using the von Neumann, Hexagonal, and Moore interaction neighborhoods. On all lattices, the comparison between the continuum and discrete data is excellent. Note that a small discontinuity develops in the continuum solution illustrated Fig. 3(c). However, we have the intriguing result that different lattices lead to different diffusivity functions $D(C)$, through different values of β in Eq. (11). This means that different continuum models are obtained on different lattices with the same mechanism in two-dimensions (and similarly in three dimensions).

B. Steady state results

To complement the transient simulations, we also performed a suite of steady state simulations on a two-dimensional lattice, with spacing $\Delta=1$, of size 200×200 with periodic boundary conditions imposed on the horizontal boundaries. Agents moving into the vertical column at $x=0$ are removed at the end of each time step giving $C=0$ in this column while agents are introduced into any empty sites in

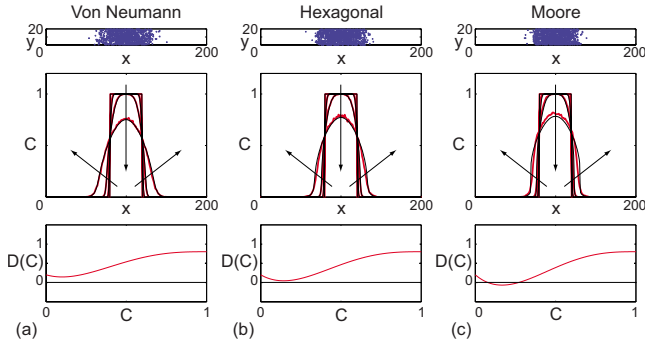


FIG. 3. (Color online) Transient results for contact-forming interactions for various cases with $s=1-p$ and $p=0.8$ for (a) square lattice with von Neumann interacting neighborhood ($k=3$, $\beta=5$), (b) hexagonal tiling ($k=3$, $\beta=7$), and (c) square lattice with Moore interacting neighborhood ($k=3$, $\beta=9$). Results in the top row show the distribution of agents in a single realization after 1000 time steps. The middle row compares the solution of the continuum model (black) and the averaged column density data (red) at $t=0, 10, 100, 1000$; arrows indicate the direction of increasing time. The bottom row shows the functional dependence of $D(C)$ on C (red) with $D(C)=0$ given by the horizontal line (black). All discrete data use $P=\Delta=\tau=1$ and averages are taken over 200 Monte Carlo realizations. Numerical solutions of the continuum models use $\delta x=0.5$ and $\delta t=0.1$. In (c), $D(C)<0$ for some values of C and the solutions of the continuum model have a discontinuity.

the vertical column at $x=l$ ($=200$ here) at the end of each time step giving $C=1$ in this column. The system was deemed to be steady when the change in the average occupancy of each column was below a tolerance. The continuum model for this problem is the boundary value problem

$$\frac{d}{dx}\left(D(C)\frac{dC}{dx}\right)=0, \quad C(0)=0, \quad C(l)=1. \quad (16)$$

The implicit solution is given by

$$x(C)=\frac{l\int_0^C D(U)dU}{\int_0^1 D(U)dU}. \quad (17)$$

For the polynomial forms of $D(C)$ considered in this work, the integrals in Eq. (17) are straightforward to evaluate.

Figure 4(a) compares simulation data with the implicit solution Eq. (17). Here, we see similar trends previously observed in the transient results. For problems where the variation in $D(C)$ is sufficiently small, corresponding to p and s near 0.5, the match between the simulation data and the solution of the boundary value problem is very good. For more extreme values of the parameter ranges, we begin to see discrepancies between the results from the two models. In particular, for $p=0.99$, $D(C)<0$ for some values of C , and the solution given by Eq. (17) has a shock at $x=0$.

Results for the contact-maintaining interactions (where the diffusivity is always positive) are illustrated in Fig. 4(b)—they follow the same trends as those in Deroulers *et al.* [6]. We observe that the continuum model predicts the

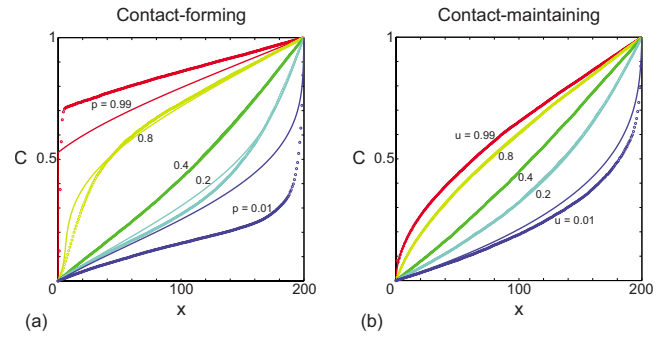


FIG. 4. (Color online) Discrete and continuum steady state results on a hexagonal tiling for (a) contact-forming interactions with $s=1-p$, for various values of p , and (b) contact-maintaining interactions with $w=1-u$ for various values of u . Discrete simulations (results given by colored circle markers) are performed on a 200×200 lattice with $P=\Delta=\tau=1$ and averages are taken over 200 Monte Carlo realizations. All simulations are performed over many time steps until the change in occupancy of all columns across the lattice is less than 0.007. The implicit solution given by Eq. (17) is shown in colored solid lines. In (a) for $p=0.99$, $D(C)<0$ for some values of C and the solution of the continuum model has a shock at $x=0$. All other plots have positive $D(C)$ and their solutions are smooth.

average discrete simulation data provided that $0.1 \leq u \leq 1$. For lower values of u the continuum and discrete models diverge.

C. Quality of fit between the discrete and continuum models

Given a set of interactions for the discrete model, it would be useful to know when the quality of fit between the average discrete data and the continuum model is good. Here, we develop a predictive tool which estimates the quality of fit.

We suggest that a useful indicator of the quality of fit is a dimensionless measure of the relative rate of change of $D(C)$ with respect to C [18]. This measure is given by

$$D^*(C)=\frac{CD'(C)}{D(C)}. \quad (18)$$

The case when $D(C)$ is constant gives $D^*(C)=0$. For this case, we know that the linear diffusion equation is an excellent fit for averaged simulation data from an exclusion process with no contact interactions [1,10].

Plots of $D(C)$ and $D^*(C)$ for contact-forming and contact-maintaining interactions are shown in Fig. 5. By comparing $D^*(C)$ shown in Fig. 5(a) with the steady state results shown in Fig. 4(a), we can deduce various trends. For p close to zero, $D^*(C)$ is largest at high values of C , matching the large discrepancies in the steady state results, while for smaller positive values of $D^*(C)$ the fit in the steady state results is good. When $D(C)$ becomes negative, we get singularities in $D^*(C)$, shocks develop in the PDE solutions and the fit between discrete and continuum models breaks down.

In general, the quality of fit between the simulation data and the relevant continuum model is acceptable when $|D^*(C)|<1$. This is supported by comparing results for the contact-maintaining interactions shown in Fig. 5(b) and

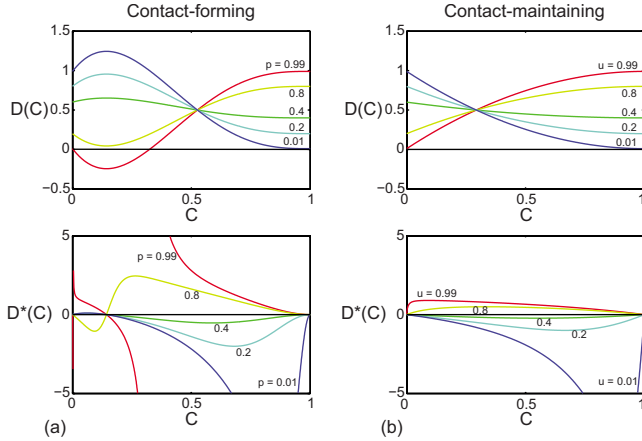


FIG. 5. (Color online) Nonlinear diffusion $D(C)$ and dimensionless measure $D^*(C)$ on hexagonal tiling for (a) contact-forming interactions with $s=1-p$ for various values of p , and (b) contact-maintaining interactions with $w=1-u$ for various values of u .

steady state results in Fig. 4(b). The graph of $D(C)$ for $u=0.01$ and $u=0.99$ are symmetric about $D(C)=0.5$ and we might expect a similar quality of fit for both these values. However, $|D^*(C)| > 1$ only for values of u close to zero; indeed the case $u=0.01$ in Fig. 4(b) gives a poor quality of fit.

There are several possible sources for the deviations, including truncation error in the Taylor series approximations used to take continuum limits, failure of assumption regarding the independence of occupancy status of lattice sites, boundary effects for the steady state results, or a combination of these issues. For example, for simulations with $D(C) < 0$, Simpson *et al.* [17] observed the formation of aggregates which means that the independence assumption is violated. Instead of identifying each of these potential sources of error, here, we prefer to propose Eq. (18) as a tool for predicting whether the continuum models developed here describe the global behavior of the system.

VI. INTERACTIONS THEN DIRECTION

In the second method, a motile agent assesses the desirability of sites in its nearest neighborhood based on contact

interactions, and a move is made with a certain biased probability weighting. Specifying the criteria and formulating the interaction rules is more complex than the methods previously described in Sec. IV since we no longer assess the direction separately. Here, we give three examples based on the one-dimensional line. As noted in Sec. IV D, these one-dimensional interactions may be implemented on colinear pairs of lattice sites in two or more dimensions, with no effect on the relevant continuum model.

We consider an exclusion process on a regular lattice with nearest neighbors $\mathcal{N}\{v\}$ of a site v , comprising $L=N/2$ colinear pairs $\{v^+, v^-\} \in \mathcal{N}\{v\}$. The site v^+ denotes the target site, while v^- denotes the neighbor in the opposite direction that the agent is moving away from. In an unbiased system with movement probability P , an agent may move to the nearest neighbor points v^+ or v^- with a equal probability $0.5P/L$. In a biased system, the occupancy status of the interacting neighborhoods $\mathcal{A}\{v^+\}$ and $\mathcal{A}\{v^-\}$ will determine the bias. Therefore, the transition probability $T(v^+|v)$ that considers a move to an arbitrary neighbor $v^+ \in \mathcal{N}\{v\}$ will also depend on the conditions in the neighborhood of the site v^- .

A. Contact-forming interaction bias

There is a specified bias in a certain direction if moving in that direction would form a contact, while moving in the opposite direction would not. If both or neither direction is contact-forming there is no bias. In the biased case, we define the probability $0.5(1+\rho)P/L$ of moving in the direction of forming a contact, and $0.5(1-\rho)P/L$ of moving in the opposite direction. The bias rules are illustrated in Fig. 6(a). The bias is independent of the occupancy of the immediately adjacent sites v^+ and v^- , shown in gray. The bias parameter satisfies $-1 \leq \rho \leq 1$. When $\rho > 0$, movements favor contact formation (attracting), whereas when $\rho < 0$, movements discourage contact formation (repelling).

The conditional transition probability for a move from v to a site $v^+ \in \mathcal{N}\{v\}$ depends on the occupancy of the contact-forming neighborhood $\mathcal{B}\{v, v^+\}$ and on the occupancy of the contact-forming neighborhood of the site in the opposite direction $\mathcal{B}\{v, v^-\}$. The transition probability is

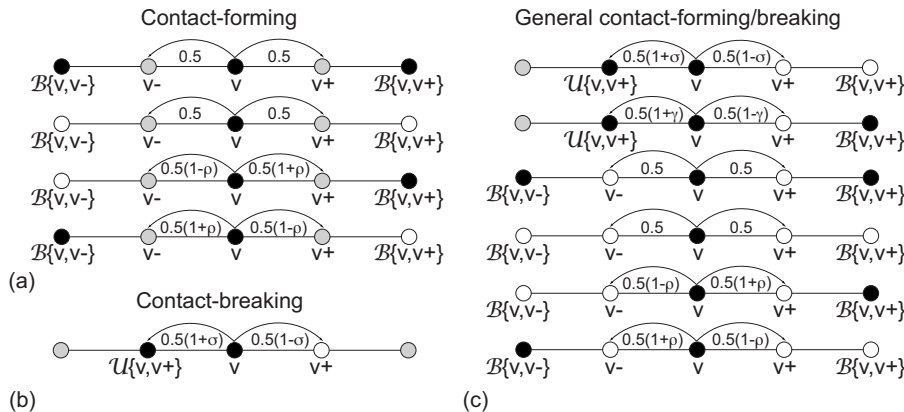


FIG. 6. Probability bias on a one-dimensional lattice. Black markers represent occupied sites, white represent unoccupied, and gray represent sites that are independent of the bias interaction rules. The factor P/L has not been shown here. (a) The contact-forming interaction probabilities, (b) the contact-breaking interaction probabilities, and (c) the general contact-forming and contact-breaking interaction probabilities. Here, $-1 \leq \rho, \sigma, \gamma \leq 1$.

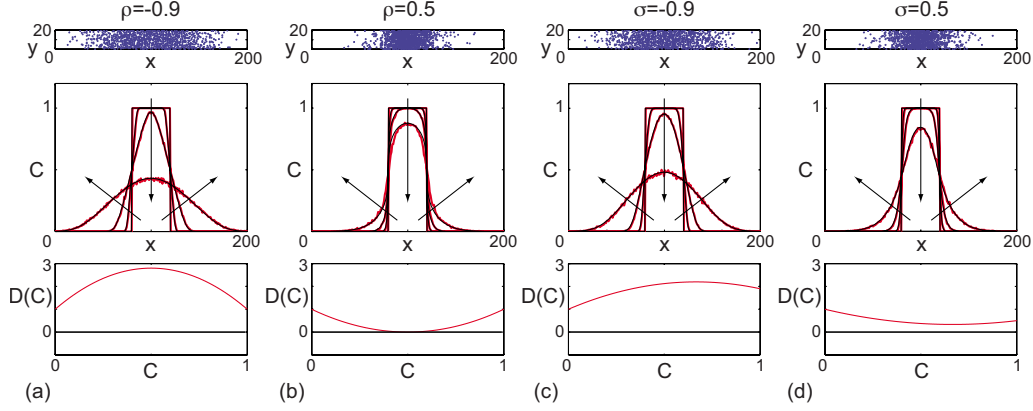


FIG. 7. (Color online) Transient results for a hexagonal tiling with biased interactions, (a) contact-forming only $\rho=-0.9$, (b) contact-forming only $\rho=0.5$, (c) contact-breaking only $\sigma=-0.9$, and (d) contact-breaking only $\sigma=0.5$. Results in the top row show the distribution of agents in a single realization after 1000 time steps. The middle row compares the solution of the continuum model (black) and the averaged column density data (red) at $t=0, 10, 100, 1000$; arrows indicate the direction of increasing time. The bottom row shows the functional dependence of $D(C)$ on C (red) with $D(C)=0$ given by the horizontal line (black). All discrete data use $P=\Delta=\tau=1$ and averages are taken over 200 Monte Carlo realizations. Numerical solutions of the continuum models use $\delta x=0.5$ and $\delta t=0.1$.

$$\begin{aligned}
 T(v^+|v) = & \frac{P}{L}(1 - \langle C_{v^+} \rangle) \left[\frac{1}{2} P_{\mathcal{B}\{v, v^+\}} P_{\mathcal{B}\{v, v^-\}} \right. \\
 & + \frac{1}{2} (1 - P_{\mathcal{B}\{v, v^+\}}) (1 - P_{\mathcal{B}\{v, v^-\}}) \\
 & + \frac{1}{2} (1 + \rho) P_{\mathcal{B}\{v, v^+\}} (1 - P_{\mathcal{B}\{v, v^-\}}) \\
 & \left. + \frac{1}{2} (1 - \rho) (1 - P_{\mathcal{B}\{v, v^+\}}) P_{\mathcal{B}\{v, v^-\}} \right]. \quad (19)
 \end{aligned}$$

In the continuum limit, we obtain Eq. (2) with

$$D(C) = 1 - 8\rho C(1 - C). \quad (20)$$

In the absence of any bias ($\rho=0$), Eq. (20) relaxes to a linear diffusivity with $D(C)=1$. Furthermore, the diffusivity has the potential to become negative for some C when $0.5 < \rho \leq 1$. These interactions were implemented on a discrete model with hexagonal tiling, with the contact-forming interaction bias applied individually to the three opposing pairs of neighboring tiles. Typical results are shown in Figs. 7(a) and 7(b) showing an excellent quality of fit. In fact, the fit is excellent for a wide range of bias parameter, namely, $\rho \in [-0.9, 0.5]$. We observed significant discrepancies between the two models for values of ρ outside this range.

B. Contact-breaking interaction bias

An agent with a single occupied interacting neighbor has two choices of movement; it can attempt to move away from the occupied site or toward it. In the latter case, the exclusion process will prevent the move, so this amounts to a choice of either moving away or not moving. However, in formulating the rules in a discrete model, we want to retain the probability of moving in the occupied direction, and allow the exclusion process to prevent the move if chance determines an attempt. We formulate a bias in terms of favoring preservation of contacts, so assign a probability of $0.5(1-\sigma)P/L$

moving away from an occupied site, and $0.5(1+\sigma)P/L$ of moving toward it, as illustrated in Fig. 6(b). The bias parameter satisfies $-1 \leq \sigma \leq 1$. When $\sigma > 0$, movements discourage contact breaking (favor contact retention), whereas when $\sigma < 0$, movements favor contact breaking (discourage contact retention).

The conditional transition probability is

$$T(v^+|v) = \frac{P}{L}(1 - \langle C_{v^+} \rangle) \left[\frac{1}{2}(1 - \sigma) P_{\mathcal{U}\{v, v^+\}} + \frac{1}{2}(1 - P_{\mathcal{U}\{v, v^+\}}) \right]. \quad (21)$$

The corresponding nonlinear diffusion function is

$$D(C) = 1 - \sigma C(4 - 3C). \quad (22)$$

We note that $D(C) < 0$ for some C when $0.75 < \sigma \leq 1$. This result was also obtained by Anguige and Schmeiser [16] in the continuum limit of a one-dimensional continuous time master equation representing cell motility with adhesion.

The contact-breaking interactions were implemented for a discrete model with hexagonal tiling, where the biasing rules were applied individually to the three opposing pairs of neighboring lattice sites. Typical results are shown in Figs. 7(c) and 7(d). Good fits were observed in the range $\sigma \in [-0.9, 0.5]$, with discrepancies outside this range, particularly above the critical value $\sigma=0.75$.

C. General contact-forming and contact-breaking interaction bias

Contact-breaking and contact-forming interactions can be combined by adding a contact-forming/contact-breaking bias γ . The rules are applied depending on one of six configurations of neighboring site occupancy, illustrated in Fig. 6(c). This results in the conditional transition probability

$$\begin{aligned}
T(v^+|v) = & \frac{P}{L}(1 - \langle C_{v^+} \rangle) \left\{ (1 - P_{\mathcal{U}\{v,v^+\}}) \left[\frac{1}{2} P_{\mathcal{B}\{v,v^+\}} P_{\mathcal{B}\{v,v^-\}} \right. \right. \\
& + \frac{1}{2} (1 - P_{\mathcal{B}\{v,v^+\}}) (1 - P_{\mathcal{B}\{v,v^-\}}) \\
& + \frac{1}{2} (1 + \rho) P_{\mathcal{B}\{v,v^+\}} (1 - P_{\mathcal{B}\{v,v^-\}}) \\
& \left. \left. + \frac{1}{2} (1 - \rho) (1 - P_{\mathcal{B}\{v,v^+\}}) P_{\mathcal{B}\{v,v^-\}} \right] + P_{\mathcal{U}\{v,v^+\}} \right. \\
& \left. \times \left[\frac{1}{2} (1 - \sigma) (1 - P_{\mathcal{B}\{v,v^+\}}) + \frac{1}{2} (1 - \gamma) P_{\mathcal{B}\{v,v^+\}} \right] \right\}. \quad (23)
\end{aligned}$$

The corresponding nonlinear diffusivity is

$$D(C) = 1 - C[8\rho(1 - C)^2 + 4\sigma(1 - C) + \gamma C]. \quad (24)$$

This is a cubic polynomial, in contrast to the quadratic polynomials found in Eq. (20) and Eq. (22).

Setting $\rho=0$ and $\gamma=\sigma$, Eq. (24) relaxes to Eq. (22) as expected. Surprisingly, Eq. (24) does not relax to Eq. (20) with an appropriate choice of parameters because the contact-forming-only case ignores the occupancy of the immediate adjacent neighbors when formulating the transition rules, whereas the general case accounts for the occupancy.

D. Quality of fit between the discrete and continuum models

Steady state simulations identical to those in Sec. V C were performed with the in-line contact-forming and contact-breaking interactions. The results obtained are consistent with those obtained previously. In summary, when $|D^*(C)| < 1$, we observed an acceptable quality of fit, whereas when $|D^*(C)| > 1$ the continuum model was unable to match the averaged discrete data.

VII. CONCLUSIONS

In this work, we have taken a biologically motivated exclusion process model, previously developed by Deroulers *et al.* [6], and generalized the agent-agent interactions to encompass contact-forming, contact-breaking, and contact-maintaining interactions. This gives rise to a suite of discrete motility models that can be implemented on arbitrary periodic lattices. For each discrete model, we use conservation arguments to arrive at a continuum model describing the collective behavior of the agent density in the system. In all cases, the continuum model is a nonlinear diffusion equation. The solution of the PDE can be either smooth or discontinuous.

There are a range of choices for implementing an exclusion process model with contact interactions. Here, we explored the possibility of either (i) choosing the direction of movement then the contact interactions or (ii) assessing the contact interactions then determining the direction of movement. We found that the first choice gives results which are generally lattice dependent. Lattice independent results were

only achieved when interactions were restricted to the line of intended movement. This is an interesting finding, which has implications for the application of such models to real systems. It seems physically unrealistic to observe a microscopic motility mechanism which gives rise to different macroscopic descriptions depending on the lattice used to discretize the spatial domain. For the second choice, we restricted our discussion to the case when movement was restricted to colinear sites, and the movement direction was biased by contact interactions. Here, the continuum model is lattice independent.

Interestingly, we observe that the average discrete and continuum models match for some parameters and fail to match for others. This is true even for the case when the diffusivity was strictly positive. There are at least two potential explanations for the divergence of the continuum and discrete models. Our assumption that the occupancy status of lattice sites is independent may be inappropriate and the Taylor series expansions may break down for some parameter values. However, our observations have allowed us to develop a simple tool which can be used to predict when the continuum-discrete comparison matches and when it fails to match.

Our work has consequences for modeling cell motility and interpreting cell motility assays. Previous approaches using nonlinear diffusion equations to represent cell motility have either used speculatively proposed forms of the nonlinear diffusivity $D(C)$ [19], or relied on fitting solutions of a nonlinear diffusion model to experimental data for a particular form of $D(C)$ [20]. Neither of these approaches considers how the macroscopic PDE model relates to individual cell movement mechanisms, nor do they consider whether these individual mechanisms were relevant in the system of interest. Similar to Deroulers *et al.* [6], our approach of proposing a biologically realistic microscopic model and then averaging the model to produce a PDE model is advantageous for several reasons. First, we have the ability to incorporate realistic cell-cell interactions from experimental data into a discrete model. By averaging the discrete model to a relevant PDE model, we avoid any speculative choice of a nonlinear diffusivity. Second, we have the ability to produce both discrete microscopic data as well as global continuum data and to compare both sets of data to experimental results, which are also likely to encompass a wide range of scales [21].

ACKNOWLEDGMENTS

This work is supported by the Australian Research Council (ARC). Kerry Landman and Matthew Simpson thank the ARC. We thank Barry Hughes for helpful discussions and feedback.

APPENDIX: NONLINEAR DIFFUSION FUNCTIONS

Table I summarizes the nonlinear diffusion function $D(C)$ arising from various one-, two- and three-dimensional lattices in Sec. IV. The parameters p , q , r , s , u , and w are motility probabilities. For the contact-maintaining interaction, u is the probability of moving if at least one maintain

TABLE I. Summary of the nonlinear diffusion function $D(C)$ arising from various lattices and interaction neighborhoods in Sec. IV. The notation is defined in the text in Appendix and Sec. IV.

Lattice and interacting neighborhood	$ \mathcal{N}\{v\} $	$ \mathcal{A}\{v\} $	$ \mathcal{M}\{v, v'\} $	$\frac{ \mathcal{B}\{v, v'\} }{ \mathcal{L}\{v, v'\} }$	Contact-maintaining interaction	General contact-forming and contact-breaking interaction	Contact-forming interaction/contact-breaking interaction
General lattice	N	b	m	k	$u+(w-u)(1-C)^m$	$r+(s-p-q+r)(1-C)^{2k}+[p(1-\beta C)+q(1+\beta C)-2r](1-C)^k$	$p+(s-p)(1+\beta C)(1-C)^k$ $q+(s-q)(1-\beta C)(1-C)^k$
Line	2	$\beta-1$ 2	0	1	N/A	$r+(s-p-q+r)(1-C)^2+[p(1-3C)+q(1+3C)-2r](1-C)$	$p+(s-p)(1+3C)(1-C)$ $q+(s-q)(1-3C)(1-C)$
Simple square (von Neumann)	4	4	0	3	N/A	$r+(s-p-q+r)(1-C)^6+[p(1-5C)+q(1+5C)-2r](1-C)^3$	$p+(s-p)(1+5C)(1-C)^3$ $q+(s-q)(1-5C)(1-C)^3$
Square with diagonals (Moore)	4	8	4	3	$u+(w-u)(1-C)^4$	$r+(s-p-q+r)(1-C)^6+[p(1-9C)+q(1+9C)-2r](1-C)^3$	$p+(s-p)(1+9C)(1-C)^3$ $q+(s-q)(1-9C)(1-C)^3$
Triangular (hexagonal tiling)	6	6	2	3	$u+(w-u)(1-C)^2$	$r+(s-p-q+r)(1-C)^6+[p(1-7C)+q(1+7C)-2r](1-C)^3$	$p+(s-p)(1+7C)(1-C)^3$ $q+(s-q)(1-7C)(1-C)^3$
Hexagonal (triangular tiling)	3	3	0	2	N/A	$r+(s-p-q+r)(1-C)^4+[p(1-4C)+q(1+4C)-2r](1-C)^2$	$p+(s-p)(1+4C)(1-C)^2$ $q+(s-q)(1-4C)(1-C)^2$
Simple cubic	6	6	0	5	N/A	$r+(s-p-q+r)(1-C)^{10}+[p(1-7C)+q(1+7C)-2r](1-C)^5$	$p+(s-p)(1+7C)(1-C)^5$ $q+(s-q)(1-7C)(1-C)^5$
Cubic with edges	6	18	8	9	$u+(w-u)(1-C)^8$	$r+(s-p-q+r)(1-C)^{18}+[p(1-19C)+q(1+19C)-2r](1-C)^9$	$p+(s-p)(1+19C)(1-C)^9$ $q+(s-q)(1-19C)(1-C)^9$
Cubic with edges and corners	6	26	16	9	$u+(w-u)(1-C)^{16}$	$r+(s-p-q+r)(1-C)^{18}+[p(1-27C)+q(1+27C)-2r](1-C)^9$	$p+(s-p)(1+27C)(1-C)^9$ $q+(s-q)(1-27C)(1-C)^9$
Face centered cubic and hexagonal close-packed	12	12	4	7	$u+(w-u)(1-C)^4$	$r+(s-p-q+r)(1-C)^{14}+[p(1-13C)+q(1+13C)-2r](1-C)^7$	$p+(s-p)(1+13C)(1-C)^7$ $q+(s-q)(1-13C)(1-C)^7$
Body centered cubic	8	8	0	7	N/A	$r+(s-p-q+r)(1-C)^{14}+[p(1-9C)+q(1+9C)-2r](1-C)^7$	$p+(s-p)(1+9C)(1-C)^7$ $q+(s-q)(1-9C)(1-C)^7$
Body centered cubic plus six orthogonals	8	14	6	7	$u+(w-u)(1-C)^6$	$r+(s-p-q+r)(1-C)^{14}+[p(1-15C)+q(1+15C)-2r](1-C)^7$	$p+(s-p)(1+15C)(1-C)^7$ $q+(s-q)(1-15C)(1-C)^7$

011903-10

neighbor is occupied, while w is the free motility probability. For all other rules, s is the free motility probability (all interacting neighborhoods unoccupied). For the general contact-forming/contact-breaking interactions, p is the probability of moving for contact-forming interactions without contact-breaking interactions, q is the probability of moving for contact-breaking interactions without contact-forming interactions, and r is the probability of moving for simultaneous contact-forming and contact-breaking interactions.

Other parameters are the number of nearest neighbors $N = |\mathcal{N}\{v\}|$, number of interacting neighbors $b = |\mathcal{A}\{v\}|$, number of contact-maintaining neighbors $m = |\mathcal{M}\{v, v'\}|$, number of contact-forming and contact-breaking neighbors $k = |\mathcal{B}\{v, v'\}| = |\mathcal{L}\{v, v'\}| = b - m - 1$. An extra parameter $\beta = b + 1$ is introduced to make the general lattice expressions more compact. When an interacting neighborhood is such that there are no contact-maintaining neighbors, the contact-maintaining rules are not applicable (denoted N/A).

-
- [1] T. M. Liggett, *Stochastic Interacting Systems: Contact, Voter and Exclusion Processes* (Springer-Verlag, Berlin, 1999).
- [2] F. Spitzer, *Adv. Math.* **5**, 246 (1970).
- [3] A. Schadschneider, *Physica A* **313**, 153 (2002).
- [4] L. M. Sander and T. S. Deisboeck, *Phys. Rev. E* **66**, 051901 (2002).
- [5] A. John, A. Schadschneider, D. Chowdhury, and K. Nishinari, *J. Theor. Biol.* **231**, 279 (2004).
- [6] C. Deroulers, M. Aubert, M. Badoual, and B. Grammaticos, *Phys. Rev. E* **79**, 031917 (2009).
- [7] M. J. Simpson, A. Merrifield, K. A. Landman, and B. D. Hughes, *Phys. Rev. E* **76**, 021918 (2007).
- [8] M. J. Simpson, K. A. Landman, and B. D. Hughes, *Bull. Math. Biol.* **71**, 781 (2009).
- [9] M. J. Simpson, K. A. Landman, and B. D. Hughes, *Physica A* **388**, 399 (2009).
- [10] M. J. Simpson, K. A. Landman, and B. D. Hughes, *Phys. Rev. E* **79**, 031920 (2009).
- [11] T. P. Witelski, *Appl. Math. Lett.* **8**, 27 (1995).
- [12] *Modeling Chemical Systems using Cellular Automata*, edited by L. B. Kier, P. G. Seybold, and C.-K. Cheng (Springer-Verlag, Amsterdam, 2005).
- [13] D. Chowdhury, A. Schadschneider, and K. Nishinari, *Phys. Life Rev.* **2**, 318 (2005).
- [14] B. D. Hughes, *Random Walks and Random Environments* (Oxford University Press, Oxford, UK, 1995), Vol. 1.
- [15] E. A. Codling, M. J. Plank, and S. Benhamou, *J. R. Soc., Interface* **5**, 813 (2008).
- [16] K. Anguige and C. Schmeiser, *J. Math. Biol.* **58**, 395 (2009).
- [17] M. J. Simpson, K. A. Landman, B. D. Hughes, A. E. Fernando, *Physica A* **389**, 1412 (2010).
- [18] V. Y. Kotlyar, *Cybern. Syst. Anal.* **35**, 653 (1999).
- [19] J. A. Sherratt, *Proc. R. Soc. London, Ser. A* **456**, 2365 (2000).
- [20] B. G. Sengers, C. P. Please, and R. O. C. Oreffo, *J. R. Soc., Interface* **4**, 1107 (2007).
- [21] B. C. Thorne, A. M. Bailey, D. W. DeSimone, and S. M. Peirce, *Birth Defects Res. C* **81**, 344 (2007).